

A Climatology of Rossby Wave Breaking along the Subtropical Tropopause

GREGORY A. POSTEL AND MATTHEW H. HITCHMAN

Department of Atmospheric and Oceanic Sciences, University of Wisconsin—Madison, Madison, Wisconsin

(Manuscript received 20 October 1997, in final form 8 April 1998)

ABSTRACT

Ten years (1986–95) of global analyses from the European Centre for Medium-Range Weather Forecasts are used to investigate the temporal and spatial distributions of Rossby wave breaking (RWB) at 350 K along the tropopause, herein defined by the ± 1.5 potential vorticity (PV) unit ($10^{-6} \text{ K m}^2 \text{ s}^{-1} \text{ kg}^{-1}$) contours. Though many studies acknowledge RWB as an important contributor to the complex of mixing processes in the atmosphere, there exists no prior climatological study of its distribution near the tropopause.

As in previous studies, RWB is identified in the global analyses by southward directed PV gradients. At 350 K, RWB along the tropopause occurs preferentially during summer over the midoceans, in relative proximity to the planetary-scale high pressure systems in the subtropics. Isentropic trajectories at 350 K show that outflow from the tops of these subtropical highs directly participates in RWB over the adjacent, downstream oceanic regions.

Two regions are highlighted in this study: the North Pacific during boreal summer and the South Atlantic during austral summer. Synoptic maps of breaking Rossby waves in these regions are provided to reveal the acute tropopause folding in the meridional plane, which characteristically accompanies RWB. The rich interaction between the tropical flow and the extratropical westerly current exhibited by these cases suggests that the subtropical highs serve as important agents in the coupling between the tropical troposphere and the extratropical stratosphere. As expected from theoretical considerations, the locations where RWB occurs most frequently, known as “surf zones,” are shown to coexist with regionally weak time-mean wind speeds and horizontal gradients of PV at 350 K.

1. Introduction

Using daily Northern Hemisphere (NH) meteorological analyses and satellite data to construct midstratosphere synoptic charts of potential vorticity (PV), McIntyre and Palmer (1983) provided the first detailed observational evidence of breaking planetary waves in the stratosphere. Over the course of several days, continental-scale tongues of relatively high PV were peeled away from the polar vortex's edge and advected (primarily isentropically) into tropical latitudes. They called this quasi-horizontal, severe distortion of PV contours “planetary wave breaking.” Planetary (or Rossby) wave breaking is characterized by the rapid (on the order of a day) and irreversible deformation of material contours. Further elucidation of the Rossby wave breaking (RWB) concept is given in McIntyre and Palmer (1984, 1985).

Analytical and numerical studies have composed consistent analogs of the observed structure of breaking Rossby waves. The theory of nonlinear critical layers,

for example, yields an analytical solution for the distribution of material contours in a critical layer, which evokes the familiar Kelvin cat's eye pattern and resembles RWB (e.g., Stewartson 1978; Warn and Warn 1978; Haynes and McIntyre 1987). Additionally, numerical modeling experiments have simulated RWB at spatial scales finer than present observational capabilities allow (e.g., Juckes and McIntyre 1987; Polvani and Plumb 1992; Waugh and Plumb 1994; Norton 1994). From these studies, it is apparent that the velocity field that attends RWB drives a cascade of motion to increasingly fine scales, wherein intensification of constituent gradients and the enhancement of transport and mixing processes occur simultaneously.

Detection of RWB's large-scale structure or form from observations remains a daunting problem since there is no unique signature or shape by which one can always identify it (McIntyre and Palmer 1985). Nonetheless, the empirical approach to studying its morphology, though unable to reveal detail due to data resolution constraints, can contribute significantly to our understanding of atmospheric chemistry issues and the maintenance of certain features of the general circulation.

Leovy et al. (1985) showed that the ozone distribution in the middle stratosphere, and thus the global distri-

Corresponding author address: Gregory A. Postel, Department of Atmospheric and Oceanic Sciences, University of Wisconsin—Madison, 1225 W. Dayton St., Madison, WI 53706.
E-mail: greg@redoubt.meteor.wisc.edu

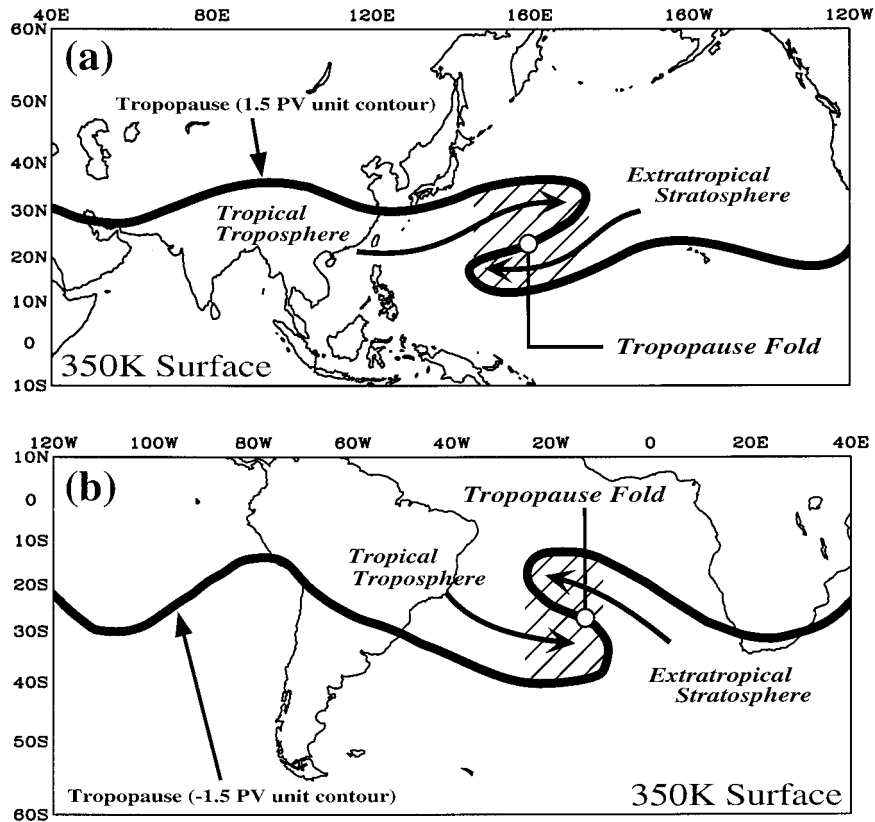


FIG. 1. Schematic of Rossby wave breaking events over (a) the North Pacific and (b) the South Atlantic, on the 350 K isentropic surface. The thick contours represent the tropopause. The hatched regions denote surf zones, where the meridional gradient of PV is regionally reversed.

bution of the total column amount of ozone, is a sensitive function of the advective processes associated with RWB. Trepte et al. (1993) implicated a role for midlatitude RWB motions in the poleward detrainment of Mount Pinatubo aerosol out of the Tropics. O'Sullivan and Hitchman (1992) used a mechanistic model of the middle atmosphere to study the interaction between Rossby waves forced at the extratropical tropopause and inertial instability in the equatorial lower mesosphere. Their results suggested that inertial instability is intimately involved in RWB in the subtropical winter mesosphere. Nakamura (1994) illustrated how deformation of the PV field associated with RWB in the upper troposphere over Europe during winter assists the development of blocked regimes. Chen (1995) suggested that the large-scale breaking of material contours, which routinely attends occluding tropospheric depressions, is primarily responsible for the vigorous cross-tropopause mass exchange observed in all seasons on and below 330 K.

This paper describes the first climatological study of RWB along the tropopause at 350 K. Since large-scale motions near the tropopause are approximately adiabatic and frictionless on synoptic timescales, an isoline of potential vorticity on an isentropic surface closely sim-

ulates a material contour. For this reason, this study employed a "PV- θ " (Hoskins 1991) view of RWB, whereby its detection was based solely on the evolution of PV on the 350 K surface.

The lack of small-scale precision in global datasets and the nonsingular appearance of breaking Rossby waves make establishing a climatology of RWB difficult. To do so, an objective definition of the process is required. Following Baldwin and Holton (1988) in their climatology of the stratospheric polar vortex and planetary wave breaking, we regard the signature of RWB as a southward-directed ("reversed") PV gradient of a selected strength. Further details of how its signature was extracted from the data are provided in section 2.

An example representative of the reversed PV gradient configurations at the tropopause, or tropopause folds, that accompany RWB is schematically depicted in Fig. 1 for each of the two focal regions in this study: the North Pacific during boreal summer and the South Atlantic during austral summer. Analogous to the often observed tropopause folding in the vertical dimension associated with occluding tropospheric cyclones, the tropopause folds detected in this study lie in the quasi-horizontal plane defined by the 350 K isentropic surface.

In this study, the tropopause is designated as the 1.5

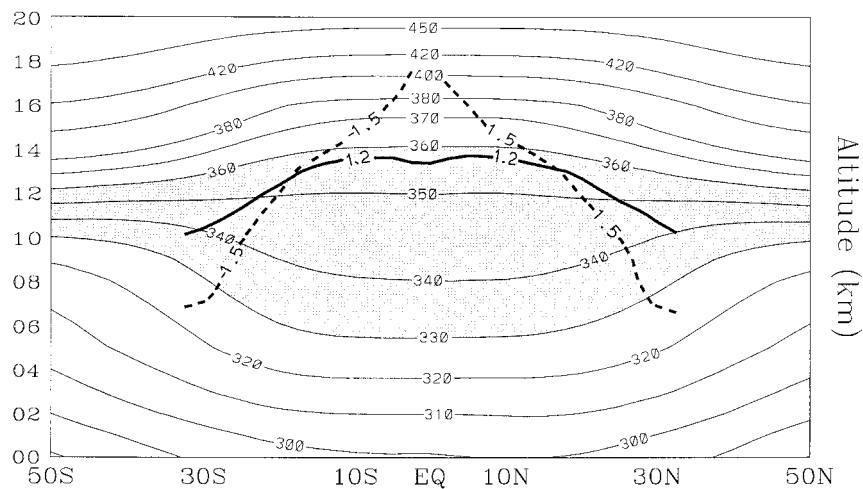


FIG. 2. Meridional cross section of the zonal-mean and time-averaged (1986–95) potential temperature (K), the 1.5 PV unit contour (thick dashed line), and the $1.2 \times 10^{-2} \text{ K m}^{-1}$ contour of the vertical gradient of potential temperature (thick solid line). The shaded region approximately delineates the “Middleworld.”

PV unit ($10^{-6} \text{ K m}^2 \text{ s}^{-1} \text{ kg}^{-1}$) contour in the NH and the -1.5 PV unit contour in the Southern Hemisphere (SH), following Hoskins et al. (1985). Though acceptable for interpreting large-scale dynamical processes in the subtropics, alternative representations of the tropopause may be more appropriate very near the equator and in midlatitudes (e.g., Hoerling et al. 1991). Figure 2 illustrates a meridional slice of the potential temperature (K) field. The ± 1.5 PV unit contours (thick dashed lines) and the $1.2 \times 10^{-2} \text{ K m}^{-1}$ contour of the vertical gradient of potential temperature (thick solid line) are superposed. In this view, the 350 K level intersects ± 1.5 PV unit contours in the subtropics, wherein they clearly establish an appropriate boundary between the troposphere and the highly stratified regime above. In the deep Tropics, the potential temperature gradient more accurately outlines the distinction between the troposphere and the stratosphere.

The tropopause folding detected in this study exemplifies interaction between the troposphere and stratosphere (e.g., Andrews et al. 1987). As shown by Fig. 2, the 350 K level lies near the center of the “Middleworld” (Hoskins 1991), which is the horizontal slab of atmosphere encompassing only those isentropes that cross the tropopause but do not intersect the earth’s surface. The selection of 350 K as the isentrope upon which RWB was detected provided a robust perspective of the RWB-induced interaction between the tropical troposphere and the extratropical stratosphere. Quantitative assessment of the net transport between the troposphere and stratosphere induced by RWB along the tropopause, which warrants diagnosis of its vertical dependence, will be reported in a later manuscript. The present purposes of isolating the frequency distribution of RWB in space and time along the tropopause at the 350 K level highlight preferred times and places in

which the tropical troposphere and the extratropical stratosphere interact.

It will be shown in section 3 that RWB at 350 K occurs most frequently during summer, over the mid-oceans. Isentropic trajectories provided in section 4 show that particularly active ducts through which RWB promotes interaction between the tropical flow and transient disturbances in the extratropical westerly current are found on the poleward and eastward edges of the upper-level, semipermanent subtropical highs. Synoptic charts of PV valid during individual RWB events, provided in section 4, reveal that the RWB distribution depends on the “fragmentation” of the subtropical highs, herein defined as a process in which chunks of tropospheric PV are stripped from the high pressure systems and advected downstream into the midlatitude stratosphere. Further insight into the RWB distributions is obtained in section 5 by examining composite summer flows near the tropopause in light of current theory. A summary and discussion are given in section 6. For reference, in the remainder of this paper, the NH summer refers to June, July, and August (JJA), and NH winter refers to December, January, and February (DJF). The SH summer (winter) refers to DJF (JJA).

2. Data and analysis methods

This study employs ten years (1986–95) of meteorological data produced by the European Centre for Medium-Range Weather Forecasts (ECMWF). Generated from operational assimilation procedures, the data consist of twice daily uninitialized globally analyzed fields of geopotential height, temperature, and horizontal wind on a $2.5^\circ \times 2.5^\circ$ grid at all standard levels in the troposphere and stratosphere. Though slight differences exist between uninitialized and initialized ECMWF ana-

lyses at the smallest horizontal scales, especially in the irrotational wind component, they nonetheless exhibit good agreement in the fields of geopotential height, wind, and temperature (e.g., Trenberth 1992; Dunkerton 1995). Trenberth (1992) provides details of the ECMWF products.

Inspection of the data showed that P ,

$$P = \frac{\theta_z}{\rho} \left\{ f - \frac{[u \cos(\phi)]_\phi}{a \cos(\phi)} + \frac{v_\lambda}{a \cos(\phi)} \right\}, \quad (1)$$

closely approximates Ertel's potential vorticity near the tropopause [cf. Andrews et al. 1987, Eq. (3.1.4)]. To compute the three-dimensional distribution of P in isobaric coordinates, second-order accurate centered difference derivatives of the wind field were used for the relative vorticity and cubic splines were used for the static stability. The isobaric distribution of P was linearly interpolated to isentropic surfaces to recover fields of PV in isentropic coordinates. Absolute values of the horizontal gradients of PV on isentropic surfaces, as shown in Fig. 10, were computed using centered differences in the zonal and meridional dimensions. Linear interpolation was also used to transform isobaric distributions of the Montgomery streamfunction and wind fields onto isentropic levels.

To limit the inclusion in the RWB climatology of tropopause folds induced by scales of motion decidedly smaller than Rossby waves, the data used by the algorithms, which tagged the tropopause folds in space and time were spectrally truncated to include only the zonal mean and first 18 zonal wavenumbers at every 2.5° lat. These data have an equivalent horizontal grid interval of 2.5° lat \times 10° long.

Three objective steps were employed to create the RWB climatology. The first was an areal search over all latitudes on the 350 K surface, at each analysis time in the 10-yr record, for a northward decrease from -1.0 to -2.0 PV units in the SH, or from $+2.0$ to $+1.0$ units in the NH, within 10° lat. If met, these criteria ensured that the meridional gradient of PV was reversed at the tropopause and associated with a strong poleward protrusion of relatively low PV from the Tropics into mid-latitudes. The locations and times that satisfied these latitudinally independent tropopause fold conditions were temporarily stored.

The second step was an areal search at each time for consecutive longitudes at which the first criterion was met. If such a series was detected, all but the westernmost location was removed from storage to ensure that the entire series was counted only once. This removed multiple tallies for a single tropopause fold whose attendant PV field deformation produced reversed PV gradients at consecutive longitudes.

The third step aimed to prevent the inclusion of reversed PV gradients associated with secluded masses of tropospheric PV in the stratosphere. In this procedure, if stratospheric PV existed at any equatorward latitude

for at least five consecutive grid points (50° of long) on a westward search from a location selected by the first two criteria, the location retained by steps one and two was discarded (see Fig. 1 for reference). This helped to remove tropopause folds associated with nearly and completely detached streams of tropospheric PV from the RWB climatology. These strips, or pieces, of PV often denoted residue of the RWB process, following the poleward and eastward surge of tropospheric air into higher latitudes.

To unambiguously link RWB along the tropopause at 350 K in the summer hemisphere to the subtropical highs, isentropic back-trajectories were derived to reveal air parcel paths during RWB. To show that air associated with RWB often comes from these high pressure systems, extraction of individual breaking waves from the tropopause fold distribution that defined the climatology was required. Owing to its transient nature, a single breaking wave may induce RWB (folds in the tropopause) at irregularly distributed locations in space and time. Since the three automated steps outlined above were unable to sequester individual breaking waves, this study employed an additional subjective visual screening of the PV field evolution associated with each tropopause fold in the climatology to retain one fold per breaking Rossby wave event. The location and time of the fold that denoted the inception of a single event were preserved.

For each breaking wave detected, a set of five trajectories was derived from the 350 K wind field, assuming adiabatic flow, using the twice daily ECMWF data on the $2.5^\circ \times 2.5^\circ$ grid. A "central" parcel was initialized at the grid point and time where the associated tropopause fold was tagged, and four additional parcels were initialized at the same time at locations 5° lat and 5° long away from the central grid point (see Fig. 7 for illustrations of these configurations). Each set was integrated backward in time for 7 days in 1-h increments using a fourth-order Runge-Kutta scheme, which employed a linear interpolation routine to retrieve the velocity field between analysis times.

The 350 K Montgomery streamfunction and horizontal winds, valid at the last time in the backward integration, were employed to elucidate the trajectories' histories. For the North Pacific sector, parcels that, at the last time step, were located equatorward of the highest open Montgomery streamfunction contour and between 40° and 120° E were defined to be associated with the high pressure system over southern Asia. Similarly, in the South Atlantic sector, parcels that, at the last time step, were located equatorward of the highest open Montgomery streamfunction contour between 100° and 20° W were defined to be associated with the high over South America. These open streamfunction contours served as references for the instantaneous high pressure systems on the 350 K surface. Closed contours often did not entirely encompass the anticyclonic shear associated with these systems, especially on their equa-

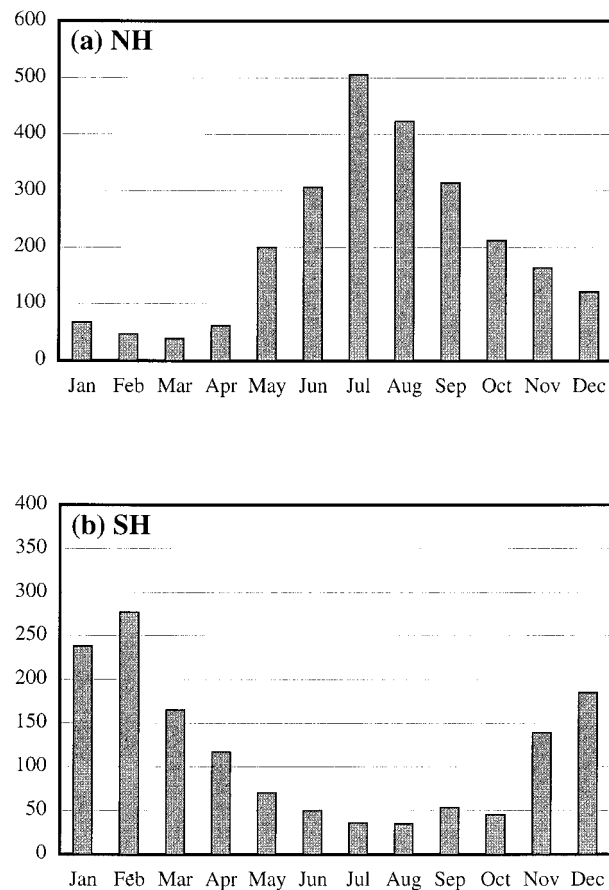


FIG. 3. Histogram of the total number of tropopause folds detected during the 1986–95 period at 350 K, as a function of month, for (a) the NH and (b) the SH.

forward flanks. In addition, closed contours did not always exist at the final time step in the trajectory algorithm, despite clear evidence of a high pressure system in other fields.

3. RWB climatology along the subtropical tropopause

Figure 3 reveals the total number of tropopause folds detected per month during the 1986–95 period. These histograms clearly illustrate the summertime predominance for RWB in both hemispheres. Figure 3a shows that in the NH, RWB-induced tropopause folds occurred most often from June–September. A month-to-month comparison reveals that RWB in the NH was detected nearly eight times more often in July than in January. The RWB frequency in the SH exhibits a similar temporal asymmetry. Figure 3b shows that RWB in the SH was most often observed during December, January, and February.

The spatial distribution of the summertime tropopause fold count accumulated during the 1986–95 period is provided in Figs. 4 (NH, JJA) and 5 (SH, DJF). Though

tropopause folds at 350 K were observed at nearly all longitudes in the northern summer, Fig. 4a strongly suggests that RWB was particularly common near the date-line and near 50°W. This is especially evident in Fig. 4b, which shows the tropopause fold count (indicated by the thick contours) and the summer-mean 150-hPa geopotential height and wind fields (superposed for later reference). According to Fig. 4b, the peaks at 180° and 50°W evident in Fig. 4a, compose two distinct regions that preferentially favor RWB: near the middle of the subtropical Pacific and Atlantic Oceans, respectively.

Figure 5a shows the austral summer tropopause fold count. The SH flow clearly favored RWB in the longitudes near 10°W, 70°E, 120°W, and to a lesser extent near 160°E. Figure 5b reveals that these peaks compose large-scale regional maxima in the RWB frequency over the South Atlantic, southern Indian, the eastern South Pacific, and to a lesser extent, extreme western portions of the South Pacific oceanic basins, respectively. As in Fig. 4b, the summer-mean 150-hPa geopotential height and wind fields are superposed on the tropopause fold count for later reference.

It has been shown thus far, that in the 1986–95 period, RWB at 350 K was detected most often during summer over the midoceans. Since the locales where tropopause folding is most common define where Rossby waves most often break, they may be thought of as regional “surf zones.” The hatched regions in Fig. 1, where breaking Rossby waves have reversed the PV gradient locally, schematically depict surf zones over the North Pacific and South Atlantic Oceans.

In the next section, direct pathways from the subtropical highs to the surf zones immediately poleward and eastward from them are uncovered. Analysis of isentropic trajectories reveals that air is rapidly transported from the high pressure systems into the surf zones during individual RWB events. This active participation in tropopause folding over the midoceans suggests that the subtropical highs’ circulations provide a favorable environment for RWB.

4. A link between the subtropical highs and RWB

According to the geopotential height and wind fields shown in Figs. 4b and 5b, the centers of the upper-level subtropical highs reside over southern Asia (90°E) and Mexico (105°W) during the northern summer and over southern Africa (25°E), northern Australia (140°E), the South Pacific (180°), and South America (60°W) during the southern summer. These large-scale anticyclonic vortices *may* be regarded as the upper flow associated with the summer monsoon circulations (e.g., Ramage 1971; Hastenrath 1991; Douglas et al. 1993). Though these systems exist over regions where observations are relatively sparse (Daley 1991), most notably in the SH, upper-air studies have long since depicted their seasonally and geographically dependent structures (e.g., Gutman and Schwerdtfeger 1965; Neyama 1968; Krish-

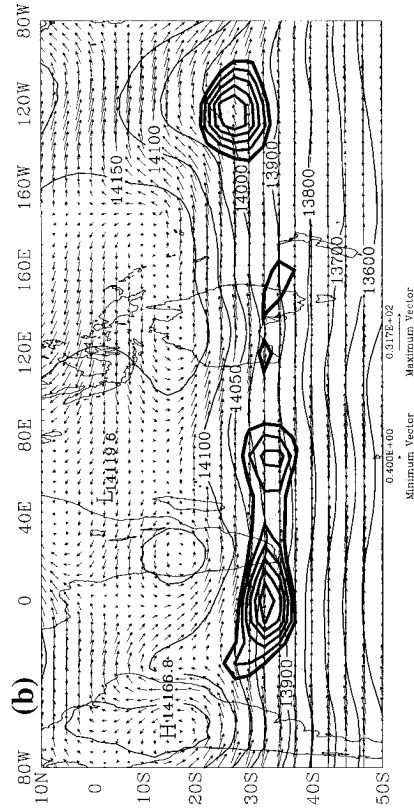
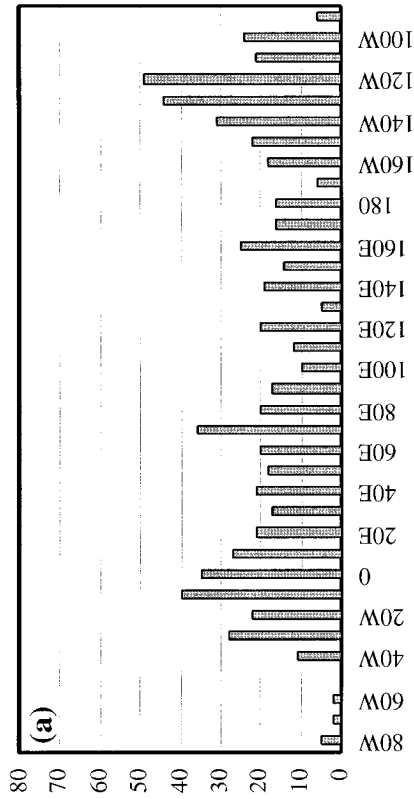


FIG. 5. Same as in Fig. 4 but for DJF in the SH. Tropopause fold count in (b) is contoured from 4 by 1.

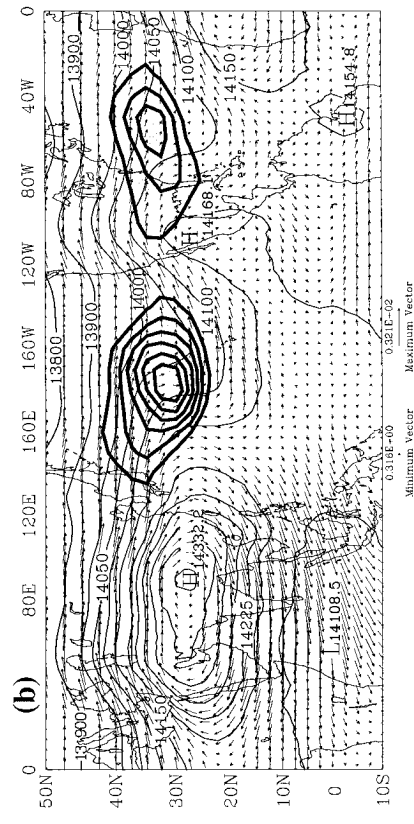
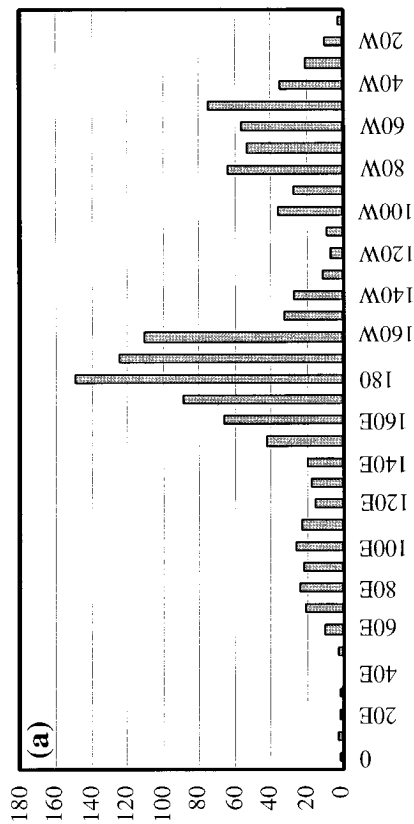


FIG. 4. Northern Hemisphere tropopause fold count summed over each JJA during 1986–95 at 350 K. (a) Histogram of its longitudinal distribution. (b) Mercator projection of its horizontal distribution shown by the unlabeled thick contours, contoured from 5 by 4; the 150-hPa geopotential heights in meters (thin labeled contours) and wind vectors ($m s^{-1}$) averaged over each JJA during 1986–95.

namurti 1970; Newell et al. 1972; Van Loon and Jenne 1972; Chu and Hastenrath 1982; Dunkerton 1995).

The circulations associated with the subtropical highs exhibit marked daily variations. Consequently, seasonal-mean views of their attendant geopotential height and wind fields present unrealistically smoothed versions of their real-time flow structures. For example, over southern Asia, daily observations (not shown) reveal that several anticyclonic circulation centers often coexist in a broad longitudinal band from roughly 40° to 140°E (e.g., Neyama 1968). Similar longitudinal asymmetries, though not as extensive, are also observed on a daily basis over South America during the austral summer. Thus, for many purposes, it is more appropriate to view the subtropical highs as a system of high pressure cells rather than a single anticyclone.

Figures 4b and 5b indicate that RWB occurred in relative proximity to the planetary-scale subtropical highs. Relatively short distances exist between the peaks in the tropopause fold count and the highest summer-mean geopotential heights associated with the subtropical highs immediately upstream. In the NH, for example, though 8200 km separates the time-mean center of the Asian high from the center of the surf zone over the North Pacific, the 14 200-m closed contour of the anticyclone system is approximately 11 500 km wide in the zonal dimension. Even less of a gap is readily apparent between the upper-level high over Mexico and the North Atlantic surf zone, given that RWB occurs relatively frequently just several grid points east and north of the highest time-mean geopotential heights. In the SH, the high pressure systems are smaller, yet the distances to the centers of the surf zones to their south and east are still several thousands of kilometers. Nonetheless, inspection of the PV field's evolution shows that these pathways are rapidly traversed by the southeastward advection of PV contours during RWB, on time-scales of the order of 1 day.

Trajectories were computed for each breaking Rossby wave event detected over the two focal regions: the North Pacific (between 140°E and 130°W) and the South Atlantic (between 40°W and 20°E). During the 10 boreal summers studied, 156 RWB events were documented over the North Pacific sector. During the 10 austral summers analyzed, 67 RWB events were documented over the South Atlantic sector.

Of the 780 trajectories initialized within the North Pacific surf zone, 25.5% were linked to the Asian anticyclone system. Of the 335 trajectories initialized within the South Atlantic surf zone, 20.9% were linked to the South American high. Figures 6a and 6b illustrate the percentage of trajectories that were coupled to the anticyclone systems as a function of the longitude of the breaking Rossby wave within which they were initialized. For example, Fig. 6a reveals that 36% of the trajectories initialized within RWB events at 140°E were traced back to the Asian high pressure system. Figure 6b shows that 40% of the trajectories initialized within

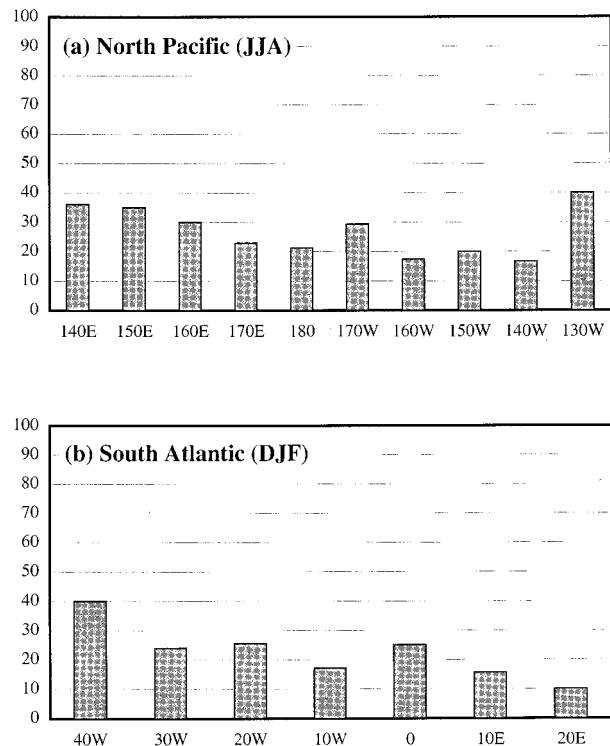


FIG. 6. Histogram of the percent of trajectories initialized within breaking Rossby waves over (a) the North Pacific and (b) the South Atlantic, which were coupled to the southern Asian and South American anticyclone systems, respectively, as a function of the longitude at which the tropopause fold was detected.

RWB events at 40°W were traced to the South American high. Both figures suggest that outflow from the subtropical highs is less likely to attend RWB over the downstream oceans the further east the events occur.

Trajectory paths for two selected RWB events are provided in Figs. 7a and 7b. These events are prototypical examples of the link between the subtropical highs and RWB. Figure 7a shows an event that occurred over the North Pacific during June 1988, and Fig. 7b illustrates another that was detected in the South Atlantic sector in December 1993. The 350 K PV field corresponding to the break time is superposed in both cases, with absolute values greater than 3 PV units shaded for clarity. The locations at which the five parcels were initialized are identified by the large dots.

In both of the cases presented in Fig. 7, only one of the five trajectories linked the surf zone to the upstream high pressure system. Maps of the streamfunction and wind fields at each analysis time (not shown) reveal that the trajectory initialized at 35°N and 175°E in the North Pacific RWB event of 1200 UTC 18 June 1988, as shown in Fig. 7a, departed the Asian high pressure system approximately 72 h earlier. The path between the South American high pressure regime and the South Atlantic surf zone was more rapidly traversed by the air parcel tagged at 35°S and 15°W (shown in Fig. 7b)

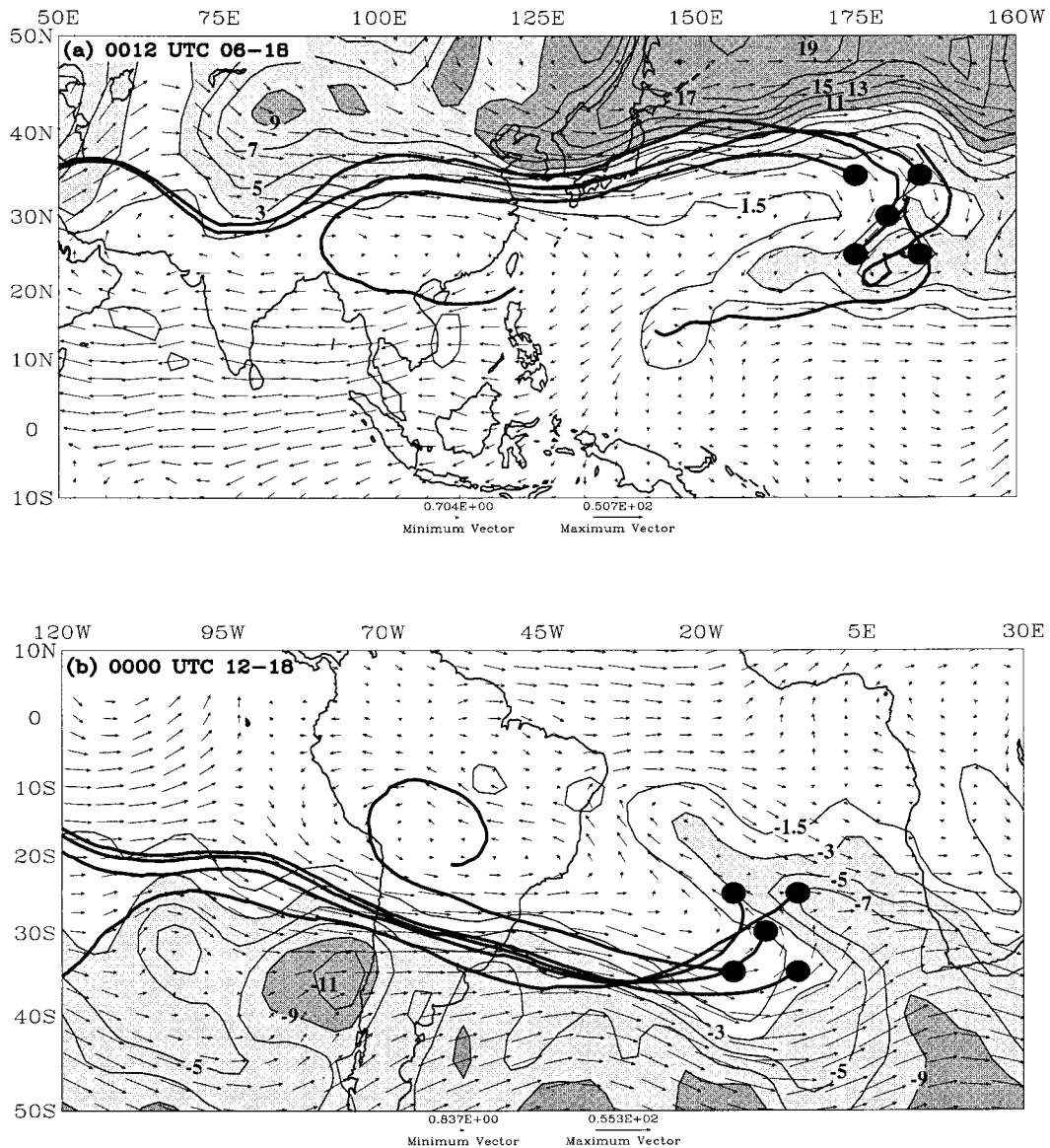


FIG. 7. Isentropic back-trajectories, PV unit contours, and wind vectors (m s^{-1}) at 350 K. Trajectory paths were initialized at the large solid dots: at $(35^{\circ}\text{N}, 175^{\circ}\text{E})$, $(35^{\circ}\text{N}, 175^{\circ}\text{W})$, $(30^{\circ}\text{N}, 180^{\circ})$, $(25^{\circ}\text{N}, 175^{\circ}\text{E})$, and $(25^{\circ}\text{N}, 175^{\circ}\text{W})$ at 1200 UTC 18 June 1988 in (a); and at $(25^{\circ}\text{S}, 15^{\circ}\text{W})$, $(25^{\circ}\text{S}, 5^{\circ}\text{W})$, $(30^{\circ}\text{S}, 10^{\circ}\text{W})$, $(35^{\circ}\text{S}, 15^{\circ}\text{W})$, and $(35^{\circ}\text{S}, 5^{\circ}\text{W})$ at 0000 UTC 18 December 1993 in (b). Winds and PV are valid at 1200 UTC 18 June 1988 in (a), and at 0000 UTC 18 December 1993 in (b). Absolute values of PV greater than 3 (9) units are lightly (heavily) shaded.

during the RWB event of 0000 UTC 18 December 1993. After 36 h, isentropic outflow from the top of the South American high attended the RWB event several thousand kilometers to its south and east.

The direct coupling that the Asian and South American anticyclonic systems exhibited with the surf zones over the North Pacific and South Atlantic Oceans, respectively, reveals that these subtropical highs participate in RWB. Figures 8 and 9 illustrate the same two RWB events shown in Fig. 7. Figures 8a–c show the North Pacific RWB event, and Figs. 9a–c illustrate the South Atlantic case.

The North Pacific sequence shows the eastward stretching of PV contours on the east flank of the anticyclonic shear associated with the well-developed Asian high pressure system, which was centered near 25°N and 100°E . On 1200 UTC 17 June, an intense westerly flow ($>40 \text{ m s}^{-1}$) existed along the north side of the Asian high with relatively vigorous northeasterly winds near 20°N and 150°E . In an anticyclonic manner, these flows rapidly advected tropospheric PV eastward, and stratospheric PV toward the southwest. By 0000 UTC 20 June 1988, fragments of tropospheric air (e.g., near 165°W and 32°N), ripped from the eastern edge of

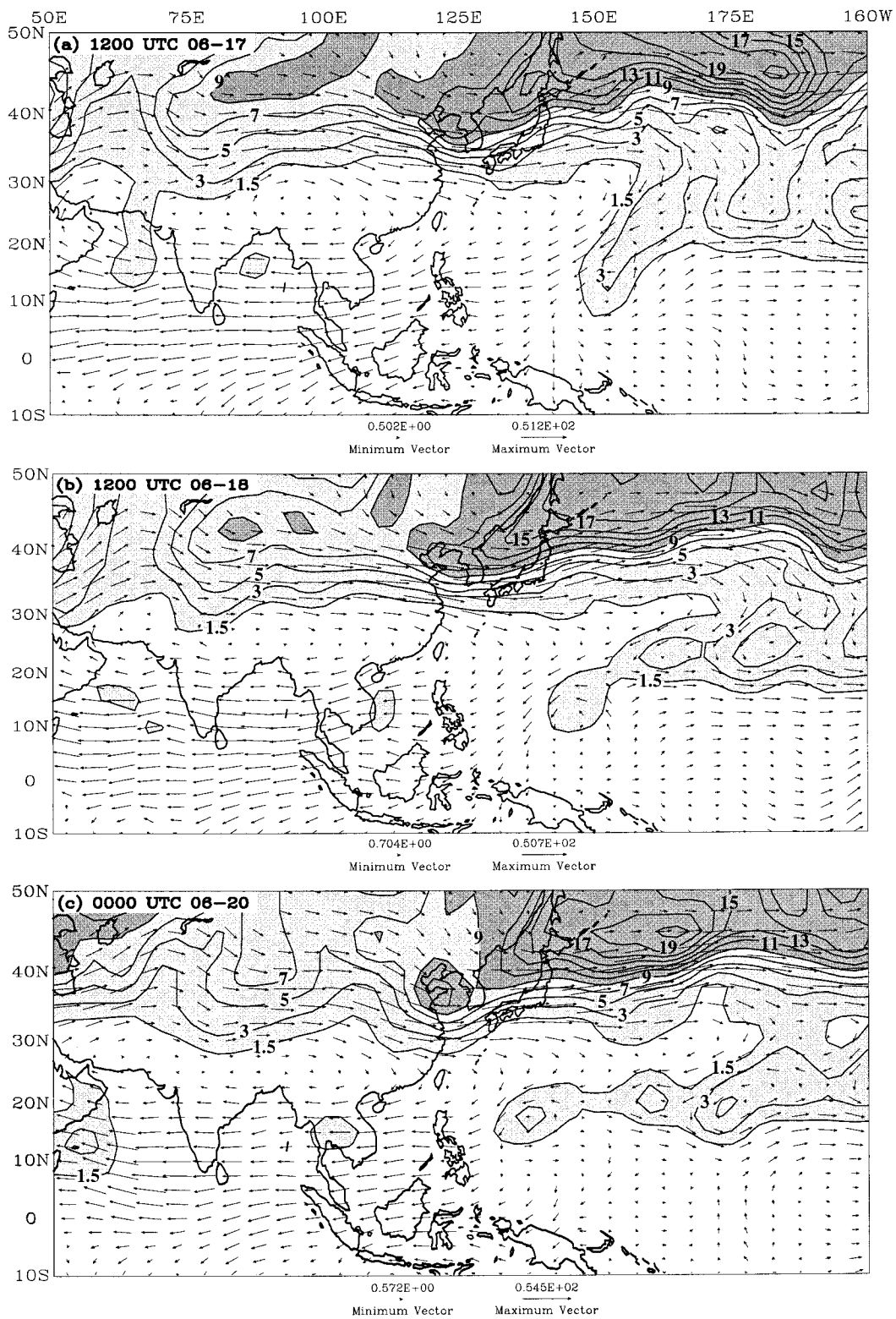


FIG. 8. PV unit contours and wind vectors (m s^{-1}) at 350 K during a RWB event over the North Pacific at (a) 1200 UTC 17 June 1988, (b) 1200 UTC 18 June 1988, and (c) 0000 UTC 20 June 1988. Absolute values of PV greater than 1.5 (9) units are lightly (heavily) shaded.

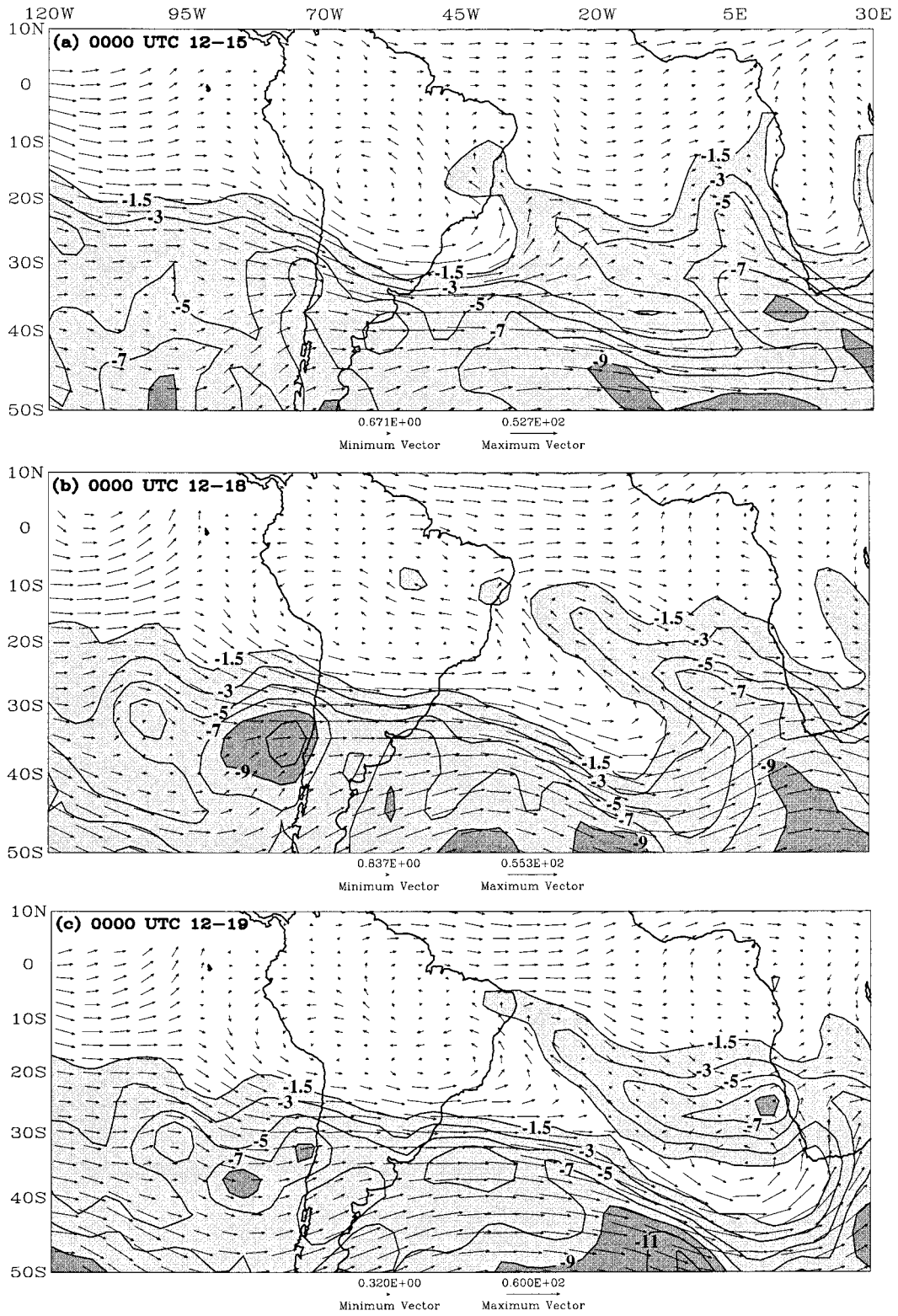


FIG. 9. Same as in Fig. 8 but over the South Atlantic at (a) 0000 UTC 15 December 1993, (b) 0000 UTC 18 December 1993, and (c) 0000 UTC 19 December 1993.

the Asian anticyclonic circulation system, appeared in the Western Hemisphere, just south of a westerly current exceeding 40 m s^{-1} . Also at that time, fragments of stratospheric PV appeared in the tropical easterly jet (e.g., Hastenrath 1991) at 15°S over southeast Asia.

Similarly, during the RWB event over the South Atlantic, exhibited by Figs. 9a–c, the rapid poleward and eastward extension of tropospheric air from the high pressure system centered over the South American interior coincided with the northwestward injection of stratospheric PV deep into the Tropics. By 0000 UTC 19 December, a synoptic-scale fragment of tropospheric air extended into the Eastern Hemisphere, equatorward of a speedy westerly wind regime and collocated with an anticyclonic gyre at 30°S and 5°E .

Both cases reveal that, in a matter of days, PV contours are pulled (and/or pushed) poleward and eastward from the subtropical highs, and folded over anticyclonically into a pattern analogous to that depicted in Fig. 1. Eventually, strips of PV are dislodged from the anticyclone systems, concluding the “fragmentation” process. By the last days shown in each sequence, air with relatively high PV (shaded), characteristic of stratospheric origin, lies adjacent to air with PV values characteristic of the tropical troposphere.

Details of the relative influences that the subtropical high pressure systems and the extratropical currents have on the instigation and sustenance of RWB events are currently under investigation by the authors. Nonetheless, it has been established herein that air streams poleward and eastward from the geographically tied high pressure systems and attends RWB in the surf zones over the downstream oceans. The air parcel trajectories shown outline corridors (schematically depicted by the curved arrows in Fig. 1) through which the tropical troposphere and extratropical stratosphere directly and rapidly interact.

5. Time-mean flows associated with the RWB distribution

The concentration of RWB at 350 K over the mid-oceans, east of the subtropical highs, from June through September in the NH and from December through March in the SH is testimony to the fact that, by certain measures, the near-tropopause flow at 350 K is more disturbed in summer than in winter. We now show that weak PV gradient and wind fields are characteristic of the summertime current over the midoceans, in relative proximity to the anticyclone systems. Theoretical considerations suggest that these flow attributes are necessary precursors to and responses of the temporal and spatial asymmetries in the RWB distributions.

a. Observed time-mean PV gradients and wind speeds

Horizontal gradients of PV on the 350 K level at the tropopause during summer are generally weaker than

those during the other seasons. For example, during the 10-yr period studied, 72% of all longitudes in the NH exhibited weaker JJA-mean gradients than those averaged over DJF. Similarly, at nearly all ($>97\%$) longitudes in the SH, summer-mean gradients were weaker than the seasonal averages for autumn, winter, and spring.

A view of the spatial distribution of the PV gradient field is provided in Fig. 10. Magnitudes of the horizontal gradients of PV (thin contours) on the 350 K surface are superposed on the RWB count (unlabeled thick contours). In the NH (as shown in Fig. 10a), two notable weaknesses in the PV gradient field protrude northeastward from the Tropics: near 180° and near 50°W . The RWB frequency maxima are collocated with the axes of relatively weak PV stratification off the east coasts of Asia and North America. In the SH (Fig. 10b) regional minima in the PV gradient field extend southeastward from the subtropical highs, shown in Fig. 5b to reside over southern Africa (25°E), the South Pacific (180°), and South America (60°W), toward the maxima in the RWB frequency over the southern Indian, southeastern Pacific, and South Atlantic Oceans. As in the NH, slices of relatively strong gradients bulge equatorward and westward on the equatorward flanks of the relatively weak gradients over the midoceans.

In addition, relatively weak winds were detected where the RWB frequencies peaked. Figure 11 illustrates summer-mean wind speeds at 350 K, averaged over the 10 yr of interest. In the northern summer (as shown in Fig. 11a), maxima in the RWB tally coexist with the poleward and eastward tilted light wind regimes over the midoceans, east and south of the time-mean jet maxima ($>20 \text{ m s}^{-1}$) observed over the east coasts of the Eurasian and North American continents. Though the summertime midlatitude winds are generally stronger in the SH than in the NH (as shown in Fig. 11b), axes of southeastward tilted corridors of relatively light winds extend over the proximate longitude bands, which hosted the RWB maxima.

b. Physical interpretations

The fact that RWB most often occurred in close proximity to chronically weak PV gradient and wind regimes follows well-explored lines of theoretical reasoning. In accordance with “PV thinking” (Hoskins et al. 1985), weakly stratified PV fields allow relatively large parcel excursions along PV gradients. The summertime flow’s preference for RWB may, in part, be attributed to the relative ease with which the subtropical highs’ outflow deforms the characteristically weak PV gradients nearby. Relatively strong PV gradients and the absence of the large-scale divergent flow associated with the summertime monsoon circulations may contribute to the dearth of RWB at 350 K during winter. In addition, observations suggest that gradients of potential vorticity are weak in weak wind regimes. Thus, as Rossby wave

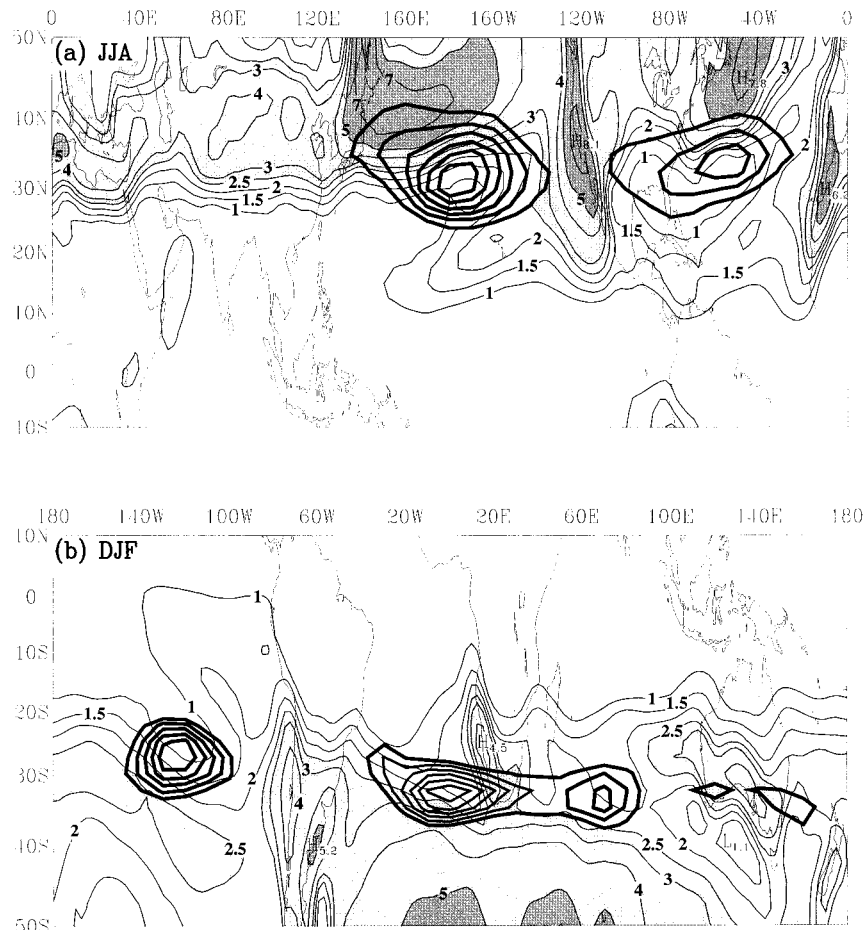


FIG. 10. Mercator projections of the magnitudes of the summer-mean horizontal gradients of PV ($10^{-12} \text{ K m s}^{-1} \text{ kg}^{-1}$), drawn by thin and labeled contours, on the 350 K surface. Values greater than $2.5 (5) \times 10^{-12} \text{ K m s}^{-1} \text{ kg}^{-1}$ are lightly (heavily) shaded. NH values, temporally averaged over each JJA in the 1986–95 period, are shown in (a). SH values, temporally averaged over each DJF in the 1986–95 period, are shown in (b). Contours (thick) of the corresponding tropopause fold counts, as shown in Figs. 4b and 5b, are superposed.

energy encounters the weak time-mean currents over the midoceans, the background flow offers relatively little resistance to wave action attempts to displace, deform, and fold over PV contours (e.g., McIntyre and Palmer 1984; Hoskins et al. 1985). Observations have shown this to be the case. For example, Nakamura (1994) showed that RWB-like deformation of the PV field occurs downstream of diffluent zones, where weak westerly flow prevails, when Rossby waves propagate into these regions from stronger westerlies upstream.

From an alternative point of view, it is almost certain that as eastward propagating Rossby waves enter the weaker ambient winds downwind of diffluent zones, differences between the waves' phase speeds and the ambient flow speeds decrease. According to critical layer theory, these locally reduced differences could in part account for the structure of the RWB distributions shown here. In fact, numerical simulations of Rossby waves propagating toward their critical latitude (e.g.,

Held and Phillips 1990), which lies where the phase and mean flow speeds match, show RWB-like PV field evolution.

On a final note, the juxtaposition of relatively strong and weak PV gradients (shown in Fig. 10) is consistent with the previously referenced numerical work, which has shown that fluid motions within RWB breaking regimes simultaneously enhance and weaken constituent gradients in nearby regions. It is likely, then, that the weakly stratified PV fields over the midoceans (as shown in Fig. 10) are at least in part a *result* of the regionally enhanced mixing associated with RWB (e.g., McIntyre and Palmer 1983). This idea naturally extends from the condition that was herein defined to be a signature of RWB, namely a reversed PV gradient.

Thus, to the extent that PV thinking, principles of critical layer theory, and results from previous RWB experiments apply to the observations presented in this paper, the time-mean flow regimes on the east sides of

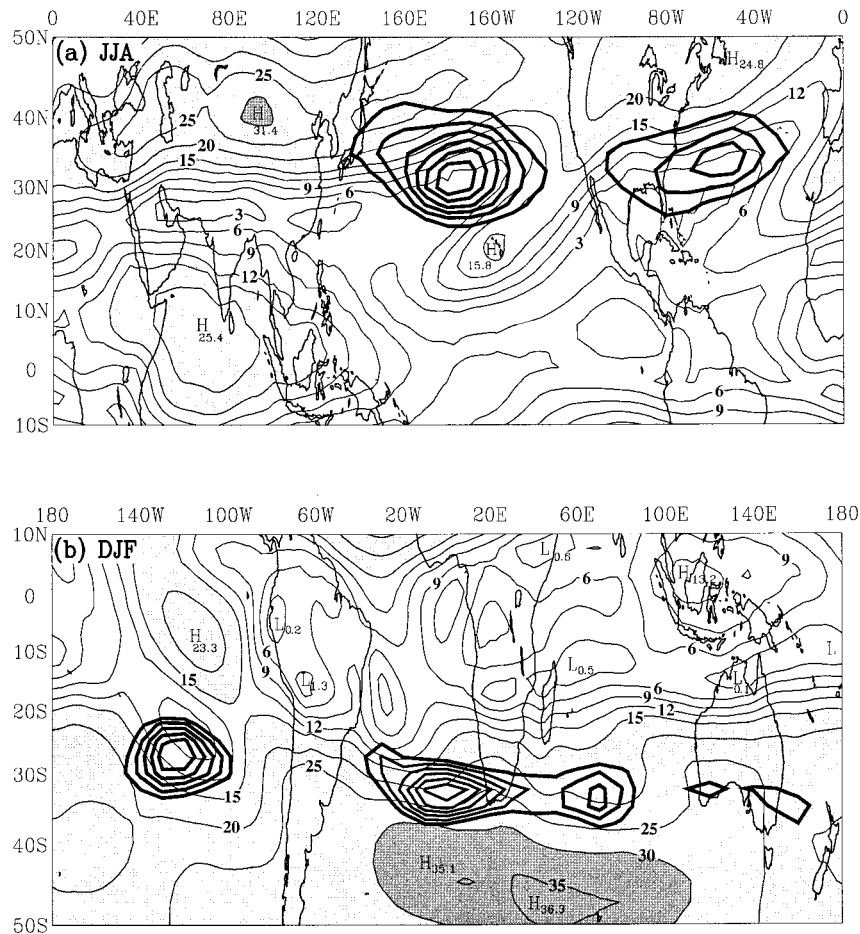


FIG. 11. Same as in Fig. 10 except wind speeds (m s^{-1}) instead of PV gradients. Wind speed contours are labeled. Values greater than 15 (30) m s^{-1} are lightly (heavily) shaded.

the subtropical highs and over the midoceans provide evidence of and for the preferential recurrence of RWB.

6. Summary and discussion

Though many studies acknowledge RWB as an important contributor to the complex of mixing processes in the atmosphere, there exists no prior survey of its spatial and temporal distributions near the tropopause. Results of this study have established that RWB induced tropopause folding at 350 K occurs preferentially over the summertime oceans, downstream of the subtropical high pressure systems. The juxtaposition of the tropical troposphere and extratropical stratosphere in these regions fosters mixing between these two very different flow regimes.

Outflow from the subtropical highs is directly involved with RWB, and participates in the troposphere-stratosphere interaction induced by the attendant tropopause folding. To this extent, troposphere-stratosphere interaction is geographically rooted to regions adjacent and downstream of the anticyclone systems, in

accordance with the tropopause fold distributions shown in Figs. 4 and 5. Implications that the east sides of the subtropical highs support such interaction via RWB are firmly supported by the aforementioned results from Chen (1995) and Dunkerton (1995). As Chen (1995) pointed out, the upper-level quasi-stationary subtropical highs are easy to break, based on their close proximity to their critical line, and should thus enhance cross-tropopause mass exchange above 340 K in the summer hemisphere.

The communication between the tropical troposphere and extratropical stratosphere focused on in this paper behaves quite differently from that described by classic teleconnection theory in which linear, quasi-rotational waves propagate away from low latitudes into the extratropics (e.g., Hoskins and Karoly 1981; Sardeshmukh and Hoskins 1988; Hoskins and Ambrizzi 1993). Though the trajectories shown in section 4 suggest that the RWB distributions are, in part, manifestations of the coupling between the divergent outflow atop the subtropical highs and the traveling eddies in the midlatitudes, the air parcel paths reveal connections that are

direct and rapid interactions, more akin to local Hadley cell overturnings (e.g., Charney 1963; Paegle et al. 1983).

The climatological results presented in section 3 were modestly sensitive to changes in the tropopause definition (TD). The monthly dependence of the RWB frequency at 350 K (as depicted in Fig. 3) varied little with increases in magnitude of the TD from ± 1.5 to ± 4.0 PV units. In each experiment, the maximum and minimum in the tropopause fold tally occurred in July (February) and March (August) in the NH (SH), respectively. However, the number of folds detected per month in both the NH and the SH decreased rapidly with increases in the TD from the ± 1.5 PV unit threshold: by a factor of 2 at the ± 2.5 PV unit TD and by a factor of 8 at the ± 4.0 PV unit TD. In addition, the locations and shapes of the surf zones (as denoted by the thick contours in Figs. 4b and 5b) were nearly unaffected by TD changes; only a slight poleward and eastward migration accompanied increases in the TD. It seems likely that the RWB frequency's limited sensitivity to TD variations (only the total tropopause fold count was notably affected) is a direct consequence of the fact that the higher TD values represent stratospheric PV unit contours, on which the wave activity amplitude has been dampened considerably during its upward propagation from the troposphere.

Alterations to the RWB climatology induced by increases in the magnitude of the minimum PV gradient (from 1.0 PV units per 10° lat to 3.0 PV units per 10° lat) required to accompany RWB mimicked those produced by changes in the TD. In particular, in both hemispheres the spatial and temporal dependencies of the RWB frequency remained nearly steady with each PV gradient change. However, the total number of tropopause folds per location (and per month) decreased with increasing gradient strength. This suggests that those RWB events associated with relatively strong reversed PV gradients occur less often, but in the usual places and at the usual times.

Though the NH and SH RWB distributions exhibit remarkable similarities, there are some noteworthy differences. Approximately twice as many tropopause folds were detected in the NH (than in the SH), despite the relative absence of RWB in multiple longitude bands (Fig. 4a). It is likely that the comparatively strong midlatitude wind speeds characteristic of the SH midlatitude flow between roughly 20° W and 100° E, evident in Fig. 11b, more broadly distributed the austral summer RWB distribution in the Eastern Hemisphere by advecting the attendant tropopause folds eastward across the South Atlantic and southern Indian Oceans. Inspection of numerous RWB events in this region (not shown) supports this notion.

It is interesting to note that the preferred regions for RWB in both the northern and southern summers appear over the middle of the oceans, near where the residence of semipermanent troughs in the upper troposphere is

well documented (e.g., Krishnamurti 1971). As shown by Figs. 7–9, RWB along the subtropical tropopause is attended by flows that pull high (in the absolute value) PV from the stratospheric reservoir equatorward into subtropical latitudes. Following PV thinking concepts, regionally high PV values in the upper troposphere, such as those that are drawn into the subtropics by the aforementioned processes, coincide with depressions in the upper-tropospheric mass field. It therefore seems possible that the fragmentation of the subtropical highs associated with RWB influences the intensity and location of the climatological upper troughs in the summer hemisphere over the oceans.

The authors are currently investigating the source(s) of the Rossby wave energy, which folds the 350 K tropopause in the regions outlined above. Perhaps Rossby waves propagating upward and equatorward from the midlatitude troposphere into the subtropics reach their critical latitude and assist the wave breaking described here.

Acknowledgments. This work was supported by NSF Grant 9120110 and NASA Grants NAG5-2722, NAS1-96030, and NAG5-2806. The ECMWF data were acquired from the National Center for Atmospheric Research, which is sponsored by the National Science Foundation.

REFERENCES

- Andrews, D. G., J. R. Holton, and C. B. Leovy, 1987: *Middle Atmosphere Dynamics*. Academic Press, 489 pp.
- Baldwin, M. P., and J. R. Holton, 1988: Climatology of the stratospheric polar vortex and planetary wave breaking. *J. Atmos. Sci.*, **45**, 1123–1142.
- Charney, J. G., 1963: A note on large-scale motions in the Tropics. *J. Atmos. Sci.*, **20**, 607–609.
- Chen, P., 1995: Isentropic cross-tropopause mass exchange in the extratropics. *J. Geophys. Res.*, **100**, 16 661–16 673.
- Chu, P.-S., and S. Hastenrath, 1982: Atlas of upper-air circulation over tropical South America. UW-Madison MET Publication No. 82.05.C1, 237 pp. [Available from University of Wisconsin—Madison, Department of Atmospheric and Oceanic Sciences, 1225 W. Dayton St., Madison, WI 53706.]
- Daley, R., 1991: *Atmospheric Data Analysis*. Cambridge University Press, 457 pp.
- Douglas, M. W., R. A. Maddox, and K. Howard, 1993: The Mexican Monsoon. *J. Climate*, **6**, 1665–1677.
- Dunkerton, T. J., 1995: Evidence of meridional motion in the summer lower stratosphere adjacent to monsoon regions. *J. Geophys. Res.*, **100**, 16 675–16 688.
- Gutman, G., and W. S. Schwerdtfeger, 1965: The role of latent and sensible heat for the development of a high pressure system over the subtropical Andes in the summer. *Meteor. Rundsch.*, **18**, 1–7.
- Hastenrath, S., 1991: *Climate Dynamics of the Tropics*. Kluwer Academic, 488 pp.
- Haynes, P. H., and M. E. McIntyre, 1987: On the representation of Rossby wave critical layers and wave breaking in zonally truncated models. *J. Atmos. Sci.*, **44**, 2359–2382.
- Held, I. M., and P. J. Phillips, 1990: A barotropic model of the interaction between the Hadley cell and a Rossby wave. *J. Atmos. Sci.*, **47**, 856–869.
- Hoerling, M. P., T. K. Schaack, and A. J. Lenzen, 1991: Global objective tropopause analysis. *Mon. Wea. Rev.*, **119**, 1816–1831.

- Hoskins, B. J., 1991: Towards a PV- θ view of the general circulation. *Tellus*, **43**, 27–35.
- , and D. J. Karoly, 1981: The steady linear response of a spherical atmosphere to thermal and orographic forcing. *J. Atmos. Sci.*, **38**, 1179–1196.
- , and T. Ambrizzi, 1993: Rossby wave propagation on a realistic longitudinally varying flow. *J. Atmos. Sci.*, **50**, 1661–1671.
- , M. E. McIntyre, and A. W. Robertson, 1985: On the use and significance of isentropic potential vorticity maps. *Quart. J. Roy. Meteor. Soc.*, **111**, 877–946.
- Juckes, M. N., and M. E. McIntyre, 1987: A high-resolution one-layer model of breaking planetary waves in the stratosphere. *Nature*, **328**, 590–596.
- Krishnamurti, T. N., 1970: Observational study of tropical upper tropospheric motion field during Northern Hemisphere summer. Tech. Rep. 70-4, The Florida State University, Tallahassee, FL, 51 pp. [Available from Florida State University, Department of Meteorology, 404 Love Building, Tallahassee, FL 32306-4250.]
- , 1971: Tropical east–west circulations during the northern summer. *J. Atmos. Sci.*, **28**, 1342–1347.
- Leovy, C. B., C.-R. Sun, M. H. Hitchman, E. E. Remsberg, J. M. Russell III, L. L. Gordley, J. C. Gille, and L. V. Lyjak, 1985: Transport of ozone in the middle stratosphere: Evidence for planetary wave breaking. *J. Atmos. Sci.*, **42**, 230–244.
- McIntyre, M. E., and T. N. Palmer, 1983: Breaking planetary waves in the stratosphere. *Nature*, **305**, 593–600.
- , and —, 1984: The “surf zone” in the stratosphere. *J. Atmos. Terrest. Phys.*, **46**, 825–849.
- , and —, 1985: A note on the general concept of wave breaking for Rossby and gravity waves. *Pure Appl. Geophys.*, **123**, 964–975.
- Nakamura, H., 1994: Rotational evolution of potential vorticity associated with a strong blocking flow configuration over Europe. *Geophys. Res. Lett.*, **21**, 2003–2006.
- Newell, R. E., J. W. Kidson, D. G. Vincent, and G. J. Boer, 1972: *The General Circulation of the Tropical Atmosphere and Interactions with Extratropical Latitudes*. Vol. 1. The MIT Press, 258 pp.
- Neyama, Y., 1968: The morphology of the subtropical anticyclone. *J. Meteor. Soc. Japan*, **46**, 431–441.
- Norton, W. A., 1994: Breaking Rossby waves in a model stratosphere diagnosed by a vortex-following coordinate system and a technique for advecting material contours. *J. Atmos. Sci.*, **51**, 654–673.
- O’Sullivan, D. J., and M. H. Hitchman, 1992: Inertial instability and Rossby wave breaking in a numerical model. *J. Atmos. Sci.*, **49**, 991–1002.
- Paegle, J., J. N. Paegle, and F. P. Lewis, 1983: Large-scale motions of the Tropics in observations and theory. *Pure Appl. Geophys.*, **121**, 947–982.
- Polvani, L. M., and R. A. Plumb, 1992: Rossby wave breaking, microbreaking, filamentation, and secondary vortex formation: The dynamics of a perturbed vortex. *J. Atmos. Sci.*, **49**, 462–476.
- Ramage, C. S., 1971: *Monsoon Meteorology*. Academic Press, 296 pp.
- Sardeshmukh, P. D., and B. J. Hoskins, 1988: The generation of global rotational flow by steady idealized tropical divergence. *J. Atmos. Sci.*, **45**, 1228–1251.
- Stewartson, K., 1978: The evolution of the critical layer of a Rossby wave. *Geophys. Astrophys. Fluid Dyn.*, **9**, 185–200.
- Trenberth, K. E., 1992: Global analyses from ECMWF and atlas of 1000 to 10 mb circulation statistics. NCAR Tech. Note NCAR/TN-373+STR., NCAR, 191 pp. [Available from UCAR Publications, P.O. Box 3000, Boulder, CO 80307.]
- Trepte, C. R., R. E. Veiga, and M. P. McCormick, 1993: The poleward dispersal of Mount Pinatubo volcanic aerosol. *J. Geophys. Res.*, **98**, 18 563–18 575.
- Van Loon, H., and R. L. Jenne, 1972: The zonal harmonic standing waves in the Southern Hemisphere. *J. Geophys. Res.*, **77**, 992–1003.
- Warn, T., and H. Warn, 1978: The evolution of a nonlinear critical level. *Stud. Appl. Math.*, **59**, 37–71.
- Waugh, D. W., and R. A. Plumb, 1994: Contour advection with surgery: A technique for investigating finescale structure in tracer transport. *J. Atmos. Sci.*, **51**, 530–540.